Tunnelling in near-integrable systems

2006 J. Phys. A: Math. Gen. 39 8283

(http://iopscience.iop.org/0305-4470/39/26/003)

INSTITUTE OF PHYSICS PUBLISHING JOURNAL OF PHYSICS A: MATHEMATICAL AND GENERAL

J. Phys. A: Math. Gen. **39** (2006) 8283–8306 doi:10.1088/0305-4470/39/26/003

Tunnelling in near-integrable systems

Graeme C Smith and Stephen C Creagh

School of Mathematical Sciences, University of Nottingham, Nottingham NG7 2RD, UK

Received 31 March 2006
Published 14 June 2006
Online at stacks.iop.org/JPhysA/39/8283

Abstract
Tunnelling rates are qualitatively different for integrable and near-integrable systems. Here a uniform result is derived which interpolates between the two regimes and is applied successfully to two-dimensional double-well and pendulum potentials. When the underlying symmetry is reflection in a single coordinate, the splitting remains positive after perturbation, but for potentials whose underlying symmetry is reflection through the origin, the splitting is predicted to oscillate as a function of a perturbation parameter, with regularly spaced zeros where tunnelling switches off.

PACS numbers: 03.65.Sq, 05.45.Mt

(Some figures in this article are in colour only in the electronic version)

1. Introduction

The classical geometry that underlies tunnelling between tori changes qualitatively when an integrable system is even slightly perturbed. Whereas in exactly integrable systems a pair of congruent invariant tori connect smoothly and form a single manifold when continued into complex phase space, those of near-integrable systems are expected to intersect transversely or even to encounter a natural boundary before any such intersection occurs in the first place. As a result, semiclassical predictions of tunnelling rates are different in each case and in particular scale differently with $\hbar$. In exactly integrable systems the energy level splitting between states supported on congruent tori is approximated in the simplest topology by the quasi-one-dimensional formula [1]

$$\Delta E^{\mathrm{int}} = \frac{\hbar\omega}{\pi}\,\mathrm{e}^{-K_0/\hbar}, \tag{1}$$

where $\mathrm{i}K_0 = \int \mathbf{p}\cdot\mathrm{d}\mathbf{q}$ is an imaginary action connecting the two real tori and ω is a frequency of motion. In d-dimensional near-integrable systems, on the other hand, a semiclassical approximation of Wilkinson's [2] (see also [3–6])

$$\Delta E^{\mathrm{ni}} = 2\left(\frac{\hbar}{2\pi}\right)^{\frac{d+1}{2}} \frac{\omega\,\mathrm{e}^{-K_0/\hbar}}{\sqrt{\mathrm{i}\{J_R, J_L\}}}, \tag{2}$$

provides an alternative structure, where J_L and J_R are actions for analytic continuations of the two real tori, which we label L and R for 'left' and 'right', and the Poisson bracket is computed on their intersection in complex phase space[1]. These two formulae are utterly different. We find in fact that the amplitude in the near-integrable version diverges in the integrable limit (where the actions J_L and J_R coincide and the Poisson bracket vanishes) and cannot be expected to describe tunnelling there. It should therefore be replaced by a uniform version just as standard WKB approximations for one-dimensional wavefunctions are replaced by Airy functions near turning points.

The purpose of this paper is twofold. First we derive a uniform result which interpolates between the integrable and near-integrable forms of tunnelling and which may in turn be useful for understanding tunnelling in mixed systems, as described below. Second, we demonstrate that, even though natural boundaries [7–9] may prevent the intersection of analytically continued tori from occurring [5] and appear formally to invalidate Wilkinson's formula, there may be approximations of the classical data which are sufficiently accurate to be used in semiclassical approximation and which are sufficiently smooth for natural boundaries to be breached and an intersection defined. In other words, Wilkinson's formula may give a good description of tunnelling even when natural boundaries prevent intersection of the exact classical tori.

In addition to being an interesting problem in its own right, understanding the mechanism for tunnelling between near-integrable tori may be of practical importance in describing tunnelling in mixed systems. Tunnelling between regular states imbedded in a mixed phase space has been the subject of much interest in recent years [10–16] and has recently been observed in experiments with cold atoms [16, 17]. In addition to the regime of *chaos-assisted tunnelling* described in [10, 11], in which tunnelling rates are enhanced by an intermediate diffusion in the stochastic regions of phase space, a mechanism of *resonance-assisted tunnelling* has been identified in [12]. In resonance-assisted tunnelling, the system tunnels between initial and final tori by hopping between resonances that lie between them. An important part of the theoretical analysis of resonance-assisted tunnelling is to estimate the coupling between tori on either side of a participating resonance, and this is achieved using quantum perturbation theory or using integrable models of tunnelling such as that for pendulum Hamiltonians described in [18]. By reaching a better understanding of tunnelling in near-integrable problems we therefore shed light on this important component of the theory of resonance-assisted tunnelling. We emphasize that by the time the perturbation parameter is large enough for the resonance-assisted mechanism to have taken over, the direct tunnelling route underlying our calculation will no longer be dominant in the overall tunnelling rate. It may still, however, control tunnelling across individual resonances and be important as a factor in the net result.

The uniform result we derive is of the form

$$\Delta E^{\mathrm{uni}}(\varepsilon) = \mathcal{M}\left(\frac{\varepsilon}{\hbar}\right) \Delta E^{\mathrm{int}}(0), \tag{3}$$

where ε is a perturbation parameter and $\Delta E^{\mathrm{int}}(0)$ is the splitting in the integrable limit $\varepsilon = 0$. The modulation function $\mathcal{M}(\varepsilon/\hbar)$ describes the transition from the integrable form of the splitting in (1) to the near-integrable form in (2). We will show that it can be written as an integral

$$\mathcal{M}(x) = \frac{1}{2\pi} \int_0^{2\pi} \mathrm{e}^{\mathrm{i}xf(\alpha)}\, \mathrm{d}\alpha, \tag{4}$$

[1] The version written by Wilkinson looks slightly different but can be rearranged to give (2) using standard identities of Hamiltonian mechanics [5].

where the phase function $f(\alpha)$ is computed using canonical perturbation theory, applied to the complexified system. When x is large, a steepest descents approximation of the integral in (4) leads to an asymptotic expression which is of the form given in (2), but with classical data approximated within perturbation theory. The important point is that Wilkinson's formula correctly captures the essential behaviour of the splitting even in generic problems where natural boundaries are expected to intervene, provided that perturbation theory leads to a sufficiently accurate solution of the Hamilton–Jacobi equation for the phase of WKB approximations. We note that similar uniform approximations for the trace formula in the vicinity of bifurcations can be arranged so that semiclassical approximations with exact classical data are recovered from the asymptotics [19–23]. This is achieved by using the exact classical data (orbit actions etc) to evaluate the arguments of the uniform approximation. The same cannot be achieved here, however, because we cannot compute the intersection of the complex tori exactly, and we can at best recover a version of (2) with additional classical approximations.

We find that the qualitative nature of $\mathcal{M}(x)$ depends on the underlying symmetry of the problem. Symmetry of the Hamiltonian with respect to reflection in a single Cartesian coordinate leads to an exponent $f(\alpha)$ which is real and $\mathcal{M}(x)$ asymptotes to an exponentially decaying or growing function of x. We find necessarily that $\mathcal{M}(x) > 0$ and this is consistent with the observation that splittings in such systems are always positive. When the underlying symmetry is inversion through a point, on the other hand, splittings can be negative—that is, the even level in a doublet can lie higher than the odd level—and $\mathcal{M}(x)$ can change sign. We find in this case that $f(\alpha)$ is generally complex and may lead to oscillatory modulation functions $\mathcal{M}(x)$. In particular, for any given doublet the theory may then predict a regular sequence of perturbation parameters at which the splitting will vanish. We therefore see a phenomenon very similar to 'coherent destruction of tunnelling' [24, 25], which has been extensively investigated in the context of driven systems in recent years, with the difference that here it is observed in autonomous problems.

We conclude this section by outlining the rest of the paper. In section 2 we provide an overview of the complex structure of exactly integrable systems and show how the splitting formula (1) can be obtained using a derivation that can also incorporate nonintegrable geometry. In section 3 canonical perturbation theory is applied to the complexified dynamics and used to approximate the classical data needed for the splitting formula. Applications to model problems with different symmetry types are considered in section 4. We conclude in section 5.

2. Complex tori and approximation of splittings

We begin by introducing notation to describe complexified tori in the integrable limit, which will help to develop complex perturbation theory later. The complexification of the multi-dimensional integrable problem is best illustrated by first considering the one-dimensional quartic oscillator. We then discuss the complexification of tori for multi-dimensional tunnelling in integrable systems. The section ends with a derivation of the splitting formula from Herring's integral, using a method that allows us to determine the leading order result when a perturbation is introduced.

2.1. The complex θ-plane for a 1D double well

Consider first the complex dynamics of a one-dimensional symmetric double well. At energies below the barrier height, the tori are one-dimensional orbits to the left and right of the barrier,

which we denote by λ_L and λ_R, respectively. We let (I, θ) be action-angle variables for the left-hand well and choose $\theta = 0$ to correspond to the inner turning point, where the orbit reflects from the barrier. The complexified torus is described by letting θ be a complex variable while keeping I real and fixed (at a value dictated by Bohr–Sommerfeld quantization).

Evolution of θ along the real axis leads to a periodic evolution on λ_L and we have, for example,

$$x(\theta) = x(\theta + 2\pi) \tag{5}$$

in a strip around the real axis. We can identify λ_L with a contour C_L on the real axis of the θ-plane running from 0 to 2π. Evolution of θ along the imaginary axis leads to periodic evolution under the potential barrier and defines a complex periodic orbit whose imaginary action appears in the exponent of the integrable splitting formula (1). Let the imaginary period be $2\mathrm{i}\Theta$, so that

$$x(\theta) = x(\theta + 2\mathrm{i}\Theta) \tag{6}$$

in a strip around the imaginary axis. We let C_0 denote a contour on the imaginary axis running from 0 to $2\mathrm{i}\Theta$ and which can be identified with the barrier-crossing periodic orbit.

Let $C_0/2$ denote a contour running from 0 to $\mathrm{i}\Theta$. Travelling up the contour $C_0/2$, we go from the inner turning point on the left-hand well to the inner turning point in the right-hand well. The overall effect is a reflection across the centre of the barrier and this extends to the symmetry

$$x(\theta + \mathrm{i}\Theta) = -x(\theta) \tag{7}$$

on the imaginary axis of the complex θ-plane. Starting at $\mathrm{i}\Theta$, evolution of θ parallel to the real axis generates real periodic motion in the right-hand well. We can therefore identify the right-hand torus λ_R with the contour

$$C_R = C_L + \mathrm{i}\Theta \tag{8}$$

in the θ-plane.

We define the *fundamental unit cell* B to be the rectangle in the complex θ-plane bordered by the contours C_L and $C_0/2$, so that the origin is at the lower left and $2\pi + \mathrm{i}\Theta$ is at the upper right. Other unit cells are obtained by translating B by integer multiples of 2π and $\mathrm{i}\Theta$. The boundary of B is a contour C obtained by concatenating $C_0/2$, C_R, $-C_0/2 + 2\pi$ and $-C_L$ (see also figure 3) and we denote by W the one-dimensional web obtained by translating the real and imaginary axes by all integer multiples of 2π and $\mathrm{i}\Theta$. The preceding discussion has established that, as θ moves along the boundary C, or more generally along the web W, $x(\theta)$ moves on the real axis in the complex x-plane, bouncing between turning points as illustrated at right in figure (1). Furthermore, the periodicity conditions in equations (5)–(7) hold for $\theta \in W$ and the symmetry

$$\mathcal{R}_x : (x, p) \mapsto (-x, -p)$$

is represented by the shift

$$\mathcal{R}_x : \theta \mapsto \theta + \mathrm{i}\Theta$$

on this web.

The arguments used to establish these conditions have been entirely dynamical and hold for any double-well potential. If we assume that the potential is analytic in a strip containing the real axis of the complex x-plane, then $x(\theta)$ and $p(\theta)$ can be extended to analytic functions on an open neighbourhood W_ϵ of the web W, on which equations (5)–(7) apply. Since a nonconstant entire function cannot be bounded on the complex plane, a nontrivial biperiodic

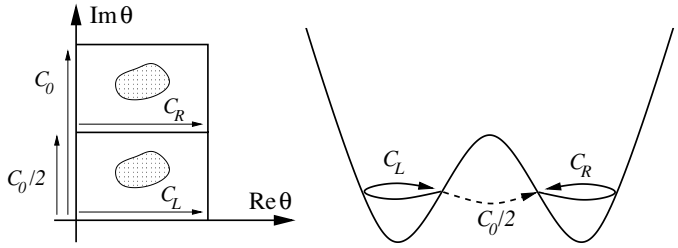

Figure 1. The contours defined in the main text are illustrated schematically.

function such as $x(\theta)$ must contain singularities in each unit cell. In the simplest case of a quartic oscillator represented by the potential $U(x) = (x^2 - 1)^2$, position and momentum are elliptic functions of θ and there is a single simple pole at the centre of each unit cell, corresponding to escape to infinity in finite imaginary time having started at one of the outer turning points. In this case the periodicity conditions in equations (5)–(7) can be extended to the whole complex plane. More generally there may be branch points inside each unit cell which prevent the biperiodicity conditions from applying globally. Crossing a branch cut may lead one to a Riemann sheet on which behaviour under translations by 2π and $i\Theta$ is entirely different, for example.

Irrespective of the nature of these singularities, however, position and momentum are single-valued, analytic and biperiodic functions of θ in the thickened web W_ϵ and this observation suffices to determine everything we need in the calculation that follows. Branch points and any other singularities can be contained within a region in the interior of each unit cell, indicated schematically by hatching in figure 1, which we exclude from our discussion. We do not require a detailed understanding of them, except possibly as an aid to evaluating certain contour integrals as will be discussed in section 4.

2.2. Complex angles in the multi-dimensional case

We will confine our discussion in this section to two-dimensional double wells which are separable in Cartesian coordinates (x, y), with a double well in the x degree of freedom and a single well in the y degree of freedom. It should be obvious how to adapt the discussion to other problems such as those based on the pendulum. For illustration we will use the Hamiltonian

$$H_0 = \tfrac{1}{2}p_x^2 + \tfrac{1}{2}p_y^2 + (x^2 - 1)^2 + \tfrac{1}{2}\Omega^2 y^2. \tag{9}$$

The real tori then project onto boxes in configuration space which are congruent with respect to reflection in x. We will show below that these are connected in a slice through real configuration space by a complex torus as illustrated schematically in figure 2. Other topologies can arise in integrable tunnelling (see [26] for example) but the main ideas are best illustrated in this simplest case.

To explain this structure in more detail, we first construct action-angle variables (I, θ) for the x degree of freedom with the angle variable being continued into a rectangular web W (or more generally a neighbourhood W_ϵ of it) in the complex plane as described in the previous section. These are augmented by action-angle variables (J, ϕ) for the y degree of freedom. Since the actions are held fixed in this discussion we will suppress them notationally and write $x(\theta)$ and $y(\phi)$. If we let θ vary over the web W, and let ϕ range over a contour C_1 going from 0 to 2π on the real axis of the ϕ-plane, three tori, two real and one complex, are covered in phase space. These are illustrated schematically in figure 2. The left and right tori

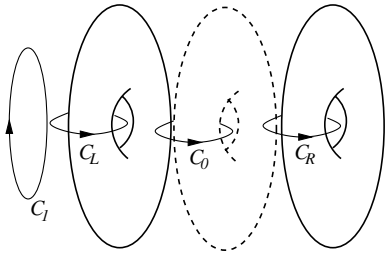

Figure 2. Schematic illustration of the real and complex tori.

correspond to $(\theta, \phi) \in C_L \times C_1$ and $(\theta, \phi) \in C_R \times C_1$, respectively. Connecting them is a complex torus on which p_x is imaginary and this corresponds to $(\theta, \phi) \in C_0 \times C_1$. Note that the tori illustrated in figure 2 represent two-dimensional subsets of a single four-dimensional complexified manifold, which is defined by letting θ and ϕ each be generically complex instead of being restricted to one-dimensional contours. The full four-dimensional manifold is difficult to visualize, however, and the restricted representation in figure 2 captures the main topological features needed for our discussion of tunnelling.

We will later treat explicitly the cases where the Hamiltonian in (9) is perturbed either by

$$H_1 = x^2 y^2 \tag{10}$$

or by

$$H_1 = xy. \tag{11}$$

It will be important when discussing splittings to establish the discrete symmetry underlying them and these two examples are representative of two distinct symmetry types that arise in two-dimensional potentials. In the case of perturbation (10), the perturbed problem is symmetric with respect to $\mathcal{R}_x : (x, y, p_x, p_y) \mapsto (-x, y, -p_x, p_y)$ and a splitting will be defined as the energy difference between states that are respectively even and odd with respect to this symmetry. It will be important later to have established that this is reflected in a symmetry with respect to the shift

$$\mathcal{R}_x : (\theta, \phi) \mapsto (\theta + \mathrm{i}\Theta, \phi)$$

in the angle variables. Perturbation (11), on the other hand, is symmetric with respect to $\mathcal{R}_{xy} : (x, y, p_x, p_y) \mapsto (-x, -y, -p_x, -p_y)$ and this corresponds in angle variables to the shift

$$\mathcal{R}_{xy} : (\theta, \phi) \mapsto (\theta + \mathrm{i}\Theta, \phi + \pi).$$

We combine both of these symmetry types in one notation by writing

$$\mathcal{R} : (\theta, \phi) \mapsto (\theta + \mathrm{i}\Theta, \phi + \sigma\pi), \tag{12}$$

where $\sigma = 0$ for problems with symmetry type $\mathcal{R} = \mathcal{R}_x$ and $\sigma = 1$ for the case $\mathcal{R} = \mathcal{R}_{xy}$.

Note that the unperturbed problem (9) is symmetric with respect to both $\mathcal{R}_x$ and $\mathcal{R}_{xy}$ and that the signs of splittings depend on which of these we adopt as the symmetry with respect to which even and odd states are defined. States that are even with respect to $\mathcal{R}_x$ may be odd with respect to $\mathcal{R}_{xy}$ and in particular the sign of the splitting may depend on which of $\mathcal{R}_x$ and $\mathcal{R}_{xy}$ we regard as being the underlying symmetry. In the case of perturbed problems, this of course is dictated by the symmetry of the perturbation itself. We will adopt the convention that $\mathcal{R}_x$ underlies the perturbation (10) and $\mathcal{R}_{xy}$ underlies the perturbation (11).

2.3. Calculating the splitting

We now derive the splitting formula for the integrable case using the same approach as used by Wilkinson to treat the nonseparable case. A simple modification of this calculation will also give us the splitting in the perturbed case. We start with a version of Herring's formula (see [2, 5])

$$\Delta E = \hbar^2 \int_\Gamma \left(\frac{\partial \psi_L^*}{\partial n} \psi_R - \psi_L^* \frac{\partial \psi_R}{\partial n} \right) \mathrm{d}s$$

which gives the splitting as an integral involving extensions into the region of evanescent decay of quasimodes ψ_L and ψ_R that are localized on the tori λ_L and λ_R, respectively. Here Γ is a contour separating the two tori in configuration space and (s, n) are orthogonal coordinates such that Γ is defined by the condition $n = 0$ and s is an arc length on Γ. The quasimodes ψ_L and ψ_R are related by the symmetry

$$\psi_R(\mathbf{x}) = \psi_L(\mathcal{R}\mathbf{x}) \tag{13}$$

that underlies the splittings, as outlined in the previous section.

Although the derivation here is in two dimensions, it is easily generalized to higher-dimensional problems. Note also that in starting with the Herring formula we have assumed that the Hamiltonian is of kinetic-plus-potential form and that λ_L and λ_R can be separated in configuration space by a contour Γ. Generalizations of the Herring formula are possible which express the splitting as an overlap on a section through phase space (see [27, 28] for example) and this would allow a derivation of the same result for more general Hamiltonians or for tori which are not separated in configuration space (such as the pendulum example described in section 4). We confine our derivation here, however, to the restricted case in order to keep the emphasis the main ideas.

We substitute WKB approximations for the localized wavefunctions. We have

$$\psi_L \approx \sum_{\text{branches}} \sqrt{\rho_L}\, \mathrm{e}^{\mathrm{i}S_L/\hbar}$$

with analogous notation for ψ_R (we assume that Maslov indices have been absorbed into the sign of ρ_L and the choice of branch for the square root). We apply this approximation in the forbidden region separating the real tori, where S_L is a complex-valued action integral over the analytic continuation of λ_L. Even though we take only the exponentially decaying branches, the others being removed by Stokes' phenomenon, a sum over branches remains because several angles ϕ will in general project to a given point in configuration space.

Let us adopt the convention that λ_L and λ_R denote the decaying branches of the complexified tori in the forbidden region—the exponentially growing branches then correspond to λ_L^* and λ_R^*.[2] It is useful to outline how these branches are understood in terms of the complex angle variables. The decaying branch λ_L of the left-hand torus is described by letting ϕ be arbitrary and letting θ descend along the imaginary axis (or at least within a neighbourhood of it) and the growing branch λ_L^* is described by letting θ ascend along it. The decaying branch λ_R of the right-hand torus can described by letting θ descend along the imaginary axis, starting from $\theta = \mathrm{i}\Theta$. In the integrable limit, λ_L^* joins smoothly with λ_R (a branch growing from the left is decaying from the right) and they are jointly described by placing θ in a neighbourhood of the imaginary axis between 0 and $\mathrm{i}\Theta$. A perturbative

[2] λ_L and λ_R extend to form a single four-dimensional complex manifold in the integrable case so distinguishing between $\lambda_L, \lambda_R, \lambda_L^*$ and λ_R^* is somewhat unnatural in a global description. From a practical point of view it is very useful however to reserve different symbols for the different branches of the complex tori corresponding to real (or nearly real) position coordinates in the forbidden region.

calculation in the next section will approximate λ_L^* and λ_R as manifolds which are distinct in the near-integrable case, but which intersect along a complex orbit. If the perturbation has symmetry, this intersection will be represented by the 'midpoint' $\theta = \mathrm{i}\Theta/2$ for a value of ϕ corresponding to $y = 0$.

As explained in the appendix, when WKB approximations for the quasimodes ψ_L and ψ_R are inserted in the Herring formula, dominant contributions in a steepest descents analysis are obtained from points on Γ corresponding to the intersection of λ_L^* with λ_R. Denote by $\tilde{\Gamma}$ the surface of section obtained by fixing the energy E in phase space and restricting $\mathbf{x} \in \Gamma$. Then, in an integrable problem, $\lambda_L^* \cap \tilde{\Gamma} \cap \lambda_R$ is topologically a one-dimensional circle and the Herring integral can be manipulated into an integral over this surface with an integration measure provided naturally by the angle variables (θ, ϕ). To describe this integral in more detail, we introduce new angle-like variables

$$\alpha = \phi - \frac{\Omega}{\omega}\theta, \qquad t = \frac{\theta}{\omega} \tag{14}$$

on each of λ_L^* and λ_R, where ω and Ω are respectively the frequencies (on the real tori) corresponding to the angles θ and ϕ. We note that α is constant on each individual orbit and is naturally used as a 2π-periodic coordinate on the circle $\lambda_L^* \cap \tilde{\Gamma} \cap \lambda_R$. Then it can be shown that in the integrable case Herring's formula becomes

$$\Delta E = \frac{\hbar\omega}{2\pi^2} \int_{\lambda_L^* \cap \tilde{\Gamma} \cap \lambda_R} \mathrm{e}^{\mathrm{i}(S_R - S_L^*)/\hbar}\, \mathrm{d}\alpha. \tag{15}$$

The action difference in the exponent takes a constant value

$$S_R - S_L^* = \oint_{C_0/2} \mathbf{p} \cdot \mathrm{d}\mathbf{q} = \mathrm{i}K_0$$

and the integrand in (15) is therefore constant, while the integral itself gives (1). We have therefore recovered the integrable form of the splitting formula.

Although there are simpler derivations of the splitting formula in the integrable case, the present approach has the advantage of extending easily to near-integrable problems. Before describing details, we note that natural boundaries may in principle arise in the exact classical dynamics which prevent straightforward WKB approximation of the quasimodes ψ_L and ψ_R from being extended as far as the dividing contour Γ. Semiclassical approximation of the splitting may nevertheless be possible even in this situation, however, if there are approximations of the complex tori that are sufficiently smooth to be continued beyond the natural boundary and which at the same time satisfy the Hamilton–Jacobi equation accurately enough to be used in WKB approximations of ψ_L and ψ_R along Γ. We show in fact that a calculation of the perturbed tori at leading order in classical perturbation theory suffices to describe the splitting quantitatively if $\varepsilon = O(\hbar)$.

We construct a leading-order semiclassical description of the splitting by approximating the amplitude in (13) by its unperturbed value and approximating the actions using first-order classical perturbation theory. Then the derivation in the appendix can be repeated to give (15), but with an action difference $S_R - S_L^*$ that is nonconstant and which leads to a nontrivial integral over α. We will show in fact that a truncated perturbation theory leads to an action difference that depends on the angle variables through α alone. That is, there is a function $f(\alpha)$ such that

$$S_R - S_L^* = \mathrm{i}K_0 + \mathrm{i}\varepsilon f(\alpha) + O(\varepsilon^2)$$

and the integral in (15) takes the form predicted in (3). If $\varepsilon/\hbar$ is large enough then we may evaluate the resulting modulation integral $\mathcal{M}(\varepsilon/\hbar)$ using the method of steepest descents

and the resulting contributions are once again identified with points in $\lambda_L^* \cap \tilde{\Gamma} \cap \lambda_R$, which are isolated in the perturbed system. The result is in fact an application of Wilkinson's formula (2) in which the classical data are approximated using classical perturbation theory. If $\varepsilon/\hbar$ is not large, on the other hand, then the modulation integral receives significant contributions from the whole range $0 < \alpha < 2\pi$ and, once integrated, produces a uniform interpolation between the integrable and Wilkinson forms of the splitting formula.

We finally point out that there is an element of redundancy in the integral (15). The contour Γ can, for example, be chosen arbitrarily in Herring's formula as long as it separates the real tori in configuration space, but we have more freedom even than that. The circle $\lambda_L^* \cap \tilde{\Gamma} \cap \lambda_R$ is in the integrable limit topologically equivalent to a loop generated on the complex torus by letting ϕ range over the contour C_1, as illustrated in figure 2. Having established that the action difference $S_R - S_L^*$ is a function of α, we see that the same result is obtained if the integral in (15) is taken over any other loop that is similarly obtained by a continuous deformation of $\lambda_L^* \cap \tilde{\Gamma} \cap \lambda_R$. We could, for example, keep θ fixed at some complex value such as $\mathrm{i}\Theta/2$ and let ϕ vary over C_1, in which case we write,

$$\Delta E = \frac{\hbar\omega}{2\pi^2} \oint_{C_1} \mathrm{e}^{\mathrm{i}(S_R - S_L^*)/\hbar}\, \mathrm{d}\phi, \tag{16}$$

where we have noted that $\mathrm{d}\alpha = \mathrm{d}\phi$ over a loop on which θ is fixed.

3. A perturbative calculation of complex tori

We now outline how the phase difference in the exponent of (15) may be computed using canonical perturbation theory. While the basic equations underlying this perturbation expansion are standard and given in textbooks ([30] for example), it should be noted that we will be interested in solving them for angle variables in the complex plane, letting θ roam around the complex web W described in section 2.1 for example. We will in particular be interested in the degree to which solutions fail to be biperiodic when extended to the complex web, and this aspect is somewhat novel. Note also that while we expect in the real case to see the toral foliation of phase space recovered at each order in perturbation theory, resonances excepted, the global complex foliation of phase space by invariant manifolds is destroyed at *leading order* and there is no global KAM theorem for complexified tori for example.

3.1. Perturbation theory for complex angles

Let

$$F_2^{L,R}(\theta, \phi, \bar{I}, \bar{J}) = \theta\bar{I} + \phi\bar{J} + G^{L,R}(\theta, \phi, \bar{I}, \bar{J})$$

be a type-2 generating function for the transformation from (θ, ϕ, I, J) to action-angle variables $(\bar{\theta}, \bar{\phi}, \bar{I}, \bar{J})$ for the perturbed system. The notation here acknowledges that there are different generating functions, labelled by L and R, for the left and right tori. We stress that in dealing with complexified tori it will be necessary to let the angle variables be complex here. Whereas $G^L(\theta, \phi, \bar{I}, \bar{J})$ should have period 2π along the real axis in the complex θ-plane, we will demand that $G^R(\theta, \phi, \bar{I}, \bar{J})$ has period 2π along the real axis translated by $\mathrm{i}\Theta$ and we will see that these different boundary conditions give rise to different solutions. In fact, in view of (12) we have

$$G^L(\theta, \phi, \bar{I}, \bar{J}) = G^R(\theta + \mathrm{i}\Theta, \phi + \sigma\pi, \bar{I}, \bar{J})$$

(the part $\theta\bar{I} + \phi\bar{J}$ is not translated because the origin of the angle coordinates is chosen on the left torus, irrespective of which solution is sought here).

Let $S_{L,R}(\mathbf{x}, \bar{I}, \bar{J})$ be the type-2 generating function transforming Cartesian to action-angle variables for a given perturbed torus and let $S^0_{L,R}(\mathbf{x}, I, J)$ be the corresponding function for the unperturbed torus. Then these functions are respectively the actions appearing in the WKB approximation of the corresponding perturbed and unperturbed quasimodes. They are related by the expression

$$\begin{aligned} S_{L,R}(\mathbf{x}, \bar{I}, \bar{J}) &= S^0_{L,R}(\mathbf{x}, I, J) + F_2^{L,R}(\theta, \phi, \bar{I}, \bar{J}) - \theta I - \phi J \\ &= S^0_{L,R}(\mathbf{x}, I, J) + (\bar{I} - I)\theta + (\bar{J} - J)\phi + G^{L,R}(\theta, \phi, \bar{I}, \bar{J}) \end{aligned}$$

(a detailed discussion of this point can be found in [4]). Using $\theta = \partial S^0_{L,R}(\mathbf{x}, I, J)/\partial I$, and the analogous expression for the remaining degree of freedom, we may approximate

$$S_{L,R}(\mathbf{x}, \bar{I}, \bar{J}) = S^0_{L,R}(\mathbf{x}, \bar{I}, \bar{J}) + G^{L,R}(\theta, \phi, \bar{I}, \bar{J}) + O(\varepsilon^2)$$

to first order in perturbation theory. We therefore find that

$$S_R - S_L^* = \mathrm{i}K_0 + \Delta G(\theta, \phi) + O(\varepsilon^2),$$

where $\mathrm{i}K_0 = S_R^0 - S_L^{0\,*}$ is the unperturbed action difference and

$$\Delta G(\theta, \phi) = G(\theta - \mathrm{i}\Theta, \phi - \sigma\pi) - G(\theta, \phi).$$

We have suppressed the action dependences in the notation since $\bar{I}$ and $\bar{J}$ will be fixed throughout the calculation by Bohr–Sommerfeld quantization conditions. We have also dropped the labels L and R, adopting from now on the convention that, where no such label is supplied, we mean generating functions to be those for the left torus. This difference will be evaluated in a neighbourhood of $\theta = \mathrm{i}\Theta/2$, corresponding to the intersection $\lambda_L^* \cap \tilde{\Gamma} \cap \lambda_R$.

We now compute the difference ΔG using canonical perturbation theory. At first order we have

$$G(\theta, \phi) = \varepsilon G_1(\theta, \phi) + O(\varepsilon^2),$$

where $G_1(\theta, \phi)$ satisfies the first-order differential equation [30]

$$\omega \frac{\partial G_1}{\partial \theta} + \Omega \frac{\partial G_1}{\partial \phi} = -V(\theta, \phi), \tag{17}$$

where we denote by

$$\{H_1\} = V(\theta, \phi) \tag{18}$$

the oscillating part of the perturbation to the Hamiltonian, expressed as a function of angle variables. Recall that ω and Ω are respectively the frequencies associated with (real dynamics of) the angles θ and ϕ. The textbook solution of this equation is obtained by first writing $V(\theta, \phi)$ as a Fourier series

$$V(\theta, \phi) = \sum_{nk} V_{nk}\, \mathrm{e}^{\mathrm{i}n\theta + \mathrm{i}k\phi}$$

and then writing the solution in a similar Fourier series form

$$G_1(\theta, \phi) = \sum_{nk} \frac{-V_{nk}}{\mathrm{i}n\omega + \mathrm{i}k\Omega}\, \mathrm{e}^{\mathrm{i}n\theta + \mathrm{i}k\phi}.$$

This form of the solution is inadequate for our purposes, however, because the Fourier series for $V(\theta, \phi)$ will converge only in a strip around the real axis in the θ-plane whereas we need to understand the solution on at least the entirety of the contour C bounding the fundamental unit cell B described in section 2.1. Note that since $V(\theta, \phi)$ (being biperiodic) must have singularities in this unit cell, the strip in which the Fourier series converges (which cannot

contain these singularities) can cover at most half of the contour $C_0/2$. In particular the midpoint $\mathrm{i}\Theta/2$ cannot be contained in the convergent strip.

We therefore start instead with a partial Fourier representation of these functions, writing

$$V(\theta,\phi)=\sum_{k=-\infty}^{\infty}V_k(\theta)\,\mathrm{e}^{\mathrm{i}k\phi} \tag{19}$$

and

$$G_1(\theta,\phi)=\sum_{k=-\infty}^{\infty}F_k(\theta)\,\mathrm{e}^{\mathrm{i}k\phi}, \tag{20}$$

so that

$$\omega\frac{\partial F_k}{\partial\theta}+\mathrm{i}k\Omega F_k(\theta)=-V_k(\theta). \tag{21}$$

A Fourier expansion in ϕ can be used because it suffices to know the solution near the real axis in the ϕ-plane but we should now solve (21) so that solutions can be extended as far as needed in the complex θ-plane.

In doing this it will be important to take into account the symmetry

$$V(\theta,\phi)=V(\theta+\mathrm{i}\Theta,\phi+\sigma\pi) \tag{22}$$

of the perturbing potential. We note that

$$\begin{aligned}\Delta G_1(\theta,\phi)&\equiv G_1(\theta-\mathrm{i}\Theta,\phi-\sigma\pi)-G_1(\theta,\phi)\\&=\sum_{k=-\infty}^{\infty}\Delta F_k(\theta)\,\mathrm{e}^{\mathrm{i}k\phi},\end{aligned}$$

where

$$\Delta F_k(\theta)=(-1)^{\sigma k}F_k(\theta-\mathrm{i}\Theta)-F_k(\theta)$$

then satisfies the equation

$$\omega\frac{\partial\Delta F_k}{\partial\theta}+\mathrm{i}k\Omega\Delta F_k=0. \tag{23}$$

Solutions to this equation are of the form

$$\Delta F_k(\theta)=A_k\,\mathrm{e}^{-\mathrm{i}k\Omega\theta/\omega}$$

so that the difference

$$\Delta G_1(\theta,\phi)=\sum_{k=-\infty}^{\infty}A_k\,\mathrm{e}^{\mathrm{i}k\phi-\mathrm{i}k\Omega\theta/\omega}=\sum_{k=-\infty}^{\infty}A_k\,\mathrm{e}^{\mathrm{i}k\alpha} \tag{24}$$

is a function of the variable α alone, and constant along orbits, as claimed in the previous section. (We could have obtained the same result by applying the method of characteristics directly to the equation for $\Delta G_1(\theta,\phi)$.)

The problem now reduces to that of determining the Fourier coefficients A_k. Before pursuing this calculation further, however, we first consider in more detail the symmetries of the perturbing potential $V(\theta,\phi)$, which will allow us to simplify the solution for G_1. In later sections these symmetries will also be useful in determining when ΔG_1 is real, generically complex or imaginary.

3.2. Symmetries of the function $V(\theta, \phi)$

In solving (17) we will make use of a number of symmetries of the right-hand side $V(\theta, \phi)$ and the corresponding Fourier coefficients $V_k(\theta)$. We collect these symmetries here for future reference.

(i) *Real period.* The real period $V(\theta + 2\pi, \phi) = V(\theta, \phi)$ leads to the condition

$$V_k(\theta + 2\pi) = V_k(\theta). \tag{25}$$

(ii) *Imaginary period.* The imaginary period expressed in (22) leads to the condition

$$V_k(\theta) = (-1)^{\sigma k} V_k(\theta + \mathrm{i}\Theta) \tag{26}$$

when expressed in the Fourier series form (this condition has already been implicitly used in deducing (23)).

(iii) *Conjugation symmetry.* Because the function $V(\theta, \phi)$ is analytically continued from a real function of real arguments, there is a conjugation symmetry

$$V^*(\theta, \phi) = V(\theta, \phi),$$

where in general we denote the conjugate $W^*(\theta, \phi)$ of a function $W(\theta, \phi)$ by $W^*(\theta, \phi) = [W(\theta^*, \phi^*)]^*$. In terms of the Fourier series this becomes

$$V_k^*(\theta) = V_{-k}(\theta), \tag{27}$$

where we use a similar convention to define $V_k^*(\theta)$.

(iv) *Reflection in y.* Some of the models we examine will possess a symmetry with respect to reflection in the y degree of freedom and this amounts to $V(\theta, \phi + \pi) = V(\theta, \phi)$ which means that

$$V_k(\theta) = 0 \qquad \text{for odd} \quad k.$$

In other models the perturbing potential will be odd with respect to inversion in y and in that case $V(\theta, \phi + \pi) = -V(\theta, \phi)$ and

$$V_k(\theta) = 0 \qquad \text{for even} \quad k.$$

These symmetries will in particular be useful in determining for which problems the action perturbation (24) is purely real, purely imaginary or generically complex. These properties are in turn important in determining the physical behaviour of the splitting and whether it oscillates or changes monotonically as a function of the perturbation parameter.

3.3. Solving for $F_k(\theta)$ using Fourier series

Recall that we compute branches of the complexified tori in the forbidden region, and the action differences between them, by computing the functions $F_k(\theta)$ as solutions of (21). We have already noted that the textbook solution

$$F_k(\theta) = \sum_{n=-\infty}^{\infty} \frac{-V_{nk}}{\mathrm{i}n\omega + \mathrm{i}k\Omega} \mathrm{e}^{\mathrm{i}n\theta} \tag{28}$$

is inadequate for our purposes because it converges only in a strip around the real axis whereas we need to know $F_k(\theta)$ along the entire rectangular web W described in section 2.1. Note that this Fourier-series solution is specific to the boundary condition,

$$F_k(\theta + 2\pi) = F_k(\theta), \tag{29}$$

on the real axis of the complex θ-plane and therefore describes the perturbed action in a neighbourhood of the left-hand real torus only. We can, however, use similar Fourier series

solutions to find solutions in other horizontal strips corresponding to complementary real tori, or in vertical strips corresponding to a tunnelling loop indicated by dashed lines in figures 1 and 2. By matching these solutions where the domains of convergence overlap we can find global solutions on the web W and determine the action difference in equation (24). The procedure to achieve this is outlined in the remainder of this section.

First, in order to extend the solution along the imaginary axis, we take advantage of the following alternative Fourier representation:

$$V_k(\theta) = \sum_{m=-\infty}^{\infty} v_{km}\, \mathrm{e}^{\kappa m\theta} \tag{30}$$

of the perturbing term in the Hamiltonian. This Fourier series is consistent with the imaginary period $V_k(\theta + 2\mathrm{i}\Theta) = V_k(\theta)$ (see (26)) if we choose

$$\kappa = \frac{\pi}{\Theta}.$$

The corresponding solution of (21), given by

$$F_k(\theta) = \begin{cases} C_k\, \mathrm{e}^{-\mathrm{i}k\Omega\theta/\omega} - \sum_{m=-\infty}^{\infty} \frac{v_{km}}{\kappa m\omega + \mathrm{i}k\Omega}\, \mathrm{e}^{\kappa m\theta} & k \neq 0, \\ C_0 - \frac{v_{00}}{\omega}\theta - \sum_{m\neq 0} \frac{v_{0m}}{\kappa m\omega}\, \mathrm{e}^{\kappa m\theta} & k = 0, \end{cases} \tag{31}$$

converges in a strip around the imaginary axis in the θ-plane and therefore describes the complexified torus in a neighbourhood of the forbidden segment of the real x-axis connecting inner turning points. Note that we have included a secular term $C_k\, \mathrm{e}^{-\mathrm{i}k\Omega\theta/\omega}$ because the relevant boundary condition is (29) and we should *not* expect the resulting solution to be periodic along the imaginary axis. In fact it is this lack of periodicity in the imaginary direction that leads to an action gap between the left- and right-continued tori and which provides the root mechanism for the energy splittings considered in this paper.

We can determine the coefficient C_k for $k \neq 0$ by comparing the solutions (28) and (31) where they both converge, at $\theta = 0$ say, giving

$$C_k = \sum_{m=-\infty}^{\infty} \left(\frac{v_{km}}{\kappa m\omega + \mathrm{i}k\Omega} \right) - \sum_{n=-\infty}^{\infty} \left(\frac{V_{kn}}{\mathrm{i}n\omega + \mathrm{i}k\Omega} \right). \tag{32}$$

The expression for $k = 0$ differs only in that the term with $m = 0$ is excluded from the first sum (and note that the function $V(\theta, \phi)$ is constructed so that $V_{00} = 0$). In matching the solution (31) to a solution (28) which is periodic along the real axis, we have extended the left-hand torus deep into the forbidden region where we expect it to intersect with the analytically continued right-hand torus. This right-hand torus is obtained by imposing the condition (29) on the horizontal line $\mathrm{Im}(\theta) = \Theta$ and, as discussed earlier, the corresponding solution for $F_k(\theta)$ is simply an upwards translation by $\mathrm{i}\Theta$ of the solution for the left-hand torus. It is represented concretely for example by the Fourier series

$$F_k^R(\theta) = F_k(\theta - \mathrm{i}\Theta) = \sum_{n=-\infty}^{\infty} \frac{-V_{nk}}{\mathrm{i}n\omega + \mathrm{i}k\Omega}\, \mathrm{e}^{\mathrm{i}n(\theta - \mathrm{i}\Theta)},$$

which converges only in a strip around the line $\mathrm{Im}(\theta) = \mathrm{i}\Theta$, or by an analogous upwards translation of the Fourier series in (31), which converges on a strip containing the imaginary axis.

The difference between these solutions is therefore

$$\begin{aligned} \Delta F_k &= (-1)^{\sigma k} F_k(\theta - \mathrm{i}\Theta) - F_k(\theta), \\ &= \begin{cases} C_k[(-1)^{\sigma k}\, \mathrm{e}^{-k\Omega\Theta/\omega} - 1]\, \mathrm{e}^{-\mathrm{i}k\Omega\theta/\omega} & k \neq 0, \\ \frac{\mathrm{i}\Theta}{\omega} v_{00} & k = 0, \end{cases} \end{aligned}$$

in the notation of section 3.1 and the net action difference demanded by the splitting formula is

$$\Delta G_1 = \frac{\mathrm{i}\Theta}{\omega} v_{00} + \sum_{k\neq 0} C_k[(-1)^{\sigma k}\,\mathrm{e}^{-k\Omega\Theta/\omega} - 1]\,\mathrm{e}^{\mathrm{i}k\phi - \mathrm{i}k\Omega\theta/\omega}. \tag{33}$$

Note that in evaluating this difference we have used the Fourier representation (31), which is convergent along the entirety of the imaginary axis.

This is an explicit result for the action difference which can be used directly in the splitting formula. It simply requires that we know the real and imaginary periods and the corresponding sets of Fourier coefficients V_{nk} and v_{km} (which could be determined numerically following a numerical integration of trajectories, for example). Although the Fourier series approach applies quite generally and is a useful practical method to obtain the action difference, some additional properties and symmetries (to be outlined in section 3.5) are not clear in the solution above and an alternative procedure is therefore outlined in the next section. We emphasize that both approaches lead ultimately to the same results. The approach in the next section is particularly useful in problems such as the quartic oscillator where the singularity structure in the complex angle plane is simple and analytic expressions can be written for the results, but the Fourier series method has the advantage of being closely related to standard approaches to real perturbation series.

3.4. Solving for $F_k(\theta)$ using an integrating factor

The differential equation (21) for $F_k(\theta)$ can also be solved using an integrating factor. We multiply through by $\mathrm{e}^{\mathrm{i}k\Omega\theta/\omega}$ and integrate, to give

$$F_k(\theta) = -\frac{\mathrm{e}^{-\mathrm{i}k\Omega\theta/\omega}}{\omega}\int_0^\theta V_k(\theta')\,\mathrm{e}^{\mathrm{i}k\Omega\theta'/\omega}\mathrm{d}\theta' + F_k(0)\,\mathrm{e}^{-\mathrm{i}k\Omega\theta/\omega}. \tag{34}$$

This result depends on the topology of the contour of integration between 0 and θ so that, although $V_k(\theta)$ is periodic along both the real and imaginary axes of the θ-plane, the function $F_k(\theta)$ is not. For example, a closed circuit around the boundary C of the fundamental unit cell described in section 2.1 leads to a nonzero result for the integral in (34), receiving contributions from poles and other singularities of $V_k(\theta)$ in the interior of the unit cell. This shows that $F_k(\theta)$ is generically not single valued on C, or more generally on the web W, and cannot then simultaneously be periodic on the real and imaginary axes.

The initial condition $F_k(0)$ can be determined by specializing (29) to $F_k(0) = F_k(2\pi)$, which, on substitution in (34), gives

$$F_k(0) = \frac{1}{\omega(1-\mathrm{e}^{2\pi\mathrm{i}k\Omega/\omega})}\int_0^{2\pi} V_k(\theta')\,\mathrm{e}^{\mathrm{i}k\Omega\theta'/\omega}\,\mathrm{d}\theta' \tag{35}$$

in the case $k \neq 0$. In the case $k = 0$ the initial condition $F_0(0)$ has no effect on the action difference $\Delta F_0(\theta)$ and can be set to zero for convenience.

Using the notation established in equation (24), the required action difference $\Delta G_1(\theta, \phi)$ is expressed in terms of Fourier coefficients A_k, which we can calculate from

$$A_k = \Delta F_k(0) = (-1)^{\sigma k} F_k(-\mathrm{i}\Theta) - F_k(0).$$

From (34) we deduce that

$$(-1)^{\sigma k} F_k(-\mathrm{i}\Theta) = -(-1)^{\sigma k}\frac{\mathrm{e}^{-k\Omega\Theta/\omega}}{\omega}\int_0^{-\mathrm{i}\Theta} V_k(\theta)\,\mathrm{e}^{\mathrm{i}k\Omega\theta/\omega}\,\mathrm{d}\theta + (-1)^{\sigma k}\,\mathrm{e}^{-k\Omega\Theta/\omega}F_k(0). \tag{36}$$

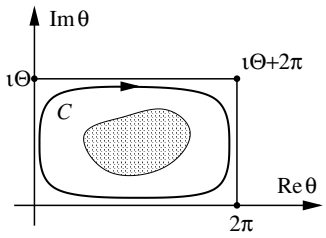

Figure 3. The action difference Fourier coefficients A_k can be expressed simply in terms of an integral over the closed contour C which runs along the boundary of the unit cell, as shown. As before, the hatched region at the centre is supposed to contain any singularities of $V_k(\theta)$.

The integral here can be simplified by first using the translation property described by (26) and then shifting the limits of the second integral in (36) by $\mathrm{i}\Theta$, to give

$$(-1)^{\sigma k}\,\mathrm{e}^{-k\Omega\Theta/\omega}\int_0^{-\mathrm{i}\Theta} V_k(\theta)\,\mathrm{e}^{\mathrm{i}k\Omega\theta/\omega}\,\mathrm{d}\theta = \int_{\mathrm{i}\Theta}^{0} V_k(\theta)\,\mathrm{e}^{\mathrm{i}k\Omega\theta/\omega}\,\mathrm{d}\theta.$$

The Fourier coefficients A_k can therefore be written as

$$A_k = \frac{1}{\omega}\int_0^{\mathrm{i}\Theta} V_k(\theta)\,\mathrm{e}^{\mathrm{i}k\Omega\theta/\omega}\,\mathrm{d}\theta + [(-1)^{\sigma k}\,\mathrm{e}^{-k\Omega\Theta/\omega} - 1]F_k(0). \tag{37}$$

When $k \neq 0$ we can manipulate this expression for A_k, after substitution of (35), into a single integral

$$A_k = \frac{1}{\omega(1-\mathrm{e}^{2\pi\mathrm{i}k\Omega/\omega})}\oint_C V_k(\theta)\,\mathrm{e}^{\mathrm{i}k\Omega\theta/\omega}\,\mathrm{d}\theta \tag{38}$$

over the contour C which runs along the boundary of the fundamental unit cell, going from 0 to $\mathrm{i}\Theta$, across to $2\pi + \mathrm{i}\Theta$, then down to 2π and finally back up to 0 again. A topologically equivalent contour is illustrated in figure 3.

When $k = 0$, equation (37) reduces directly to

$$A_0 = \frac{1}{\omega}\int_0^{\mathrm{i}\Theta} V_0(\theta)\,\mathrm{d}\theta \tag{39}$$

and this term can be interpreted in terms of averaging over real and complex tori as follows. We first recall that

$$V_0(\theta) = \langle H_1\rangle_\phi - \langle H_1\rangle_{\theta,\phi},$$

where the subscripts indicate which angles are averaged over, and then write

$$\begin{aligned} A_0 &= \frac{1}{\omega}\int_0^{\mathrm{i}\Theta}(\langle H_1\rangle_\phi - \langle H_1\rangle_{\theta,\phi})\,\mathrm{d}\theta \\ &= \frac{\mathrm{i}\Theta}{\omega}\left(\frac{1}{\mathrm{i}\Theta}\int_0^{\mathrm{i}\Theta}\langle H_1\rangle_\phi\,\mathrm{d}\theta - \langle H_1\rangle_{\theta,\phi}\right) \\ &= \mathrm{i}\tau\big(\langle H_1\rangle_{(\theta,\phi)\in C_0\times C_1} - \langle H_1\rangle_{(\theta,\phi)\in C_L\times C_1}\big), \end{aligned} \tag{40}$$

where in the last line we have substituted

$$\tau = \frac{\Theta}{\omega},$$

where $\mathrm{i}\tau$ is the imaginary time taken for a complex trajectory to pass from one barrier turning point to the other. That is, A_0 is proportional to the difference between an average of $H_1(\theta,\phi)$

over the complex torus, illustrated by the dashed part of figure 2, and an average of $H_1(\theta, \phi)$ over one of the real tori.

Note that in the notation used for Fourier series, $v_{00} = \langle H_1 \rangle_{(\theta,\phi)\in C_0\times C_1} - \langle H_1 \rangle_{(\theta,\phi)\in C_L\times C_1}$ and this expression for A_0 coincides with the first term in (33). Likewise, if we evaluate the integral in (38) by substituting the appropriate Fourier series for $V_k(\theta)$ along each of the four segments of C (namely (30), its equivalent along the real axis and their respective translations by 2π and $\mathrm{i}\Theta$) then we recover the Fourier coefficients in the sum in (33). Therefore the final results of this section are equivalent to those of Fourier series approach, although arrived at from a different point of view.

3.5. Implications of symmetry

From the solution outlined in section 3.4, we now show that the first-order action difference $\Delta G_1(\theta, \phi)$ in (24) may be either purely real or purely imaginary, according to the underlying symmetry of the problem. We achieve this by first using the conjugation and translation symmetries discussed in section 3.2 to show that, for either of the underlying symmetry types, we have

$$A_k^* = -(-1)^{\sigma k}\, \mathrm{e}^{k\Omega\Theta/\omega} A_{-k}. \tag{41}$$

This relationship can be obtained for $k \neq 0$ by conjugating the integral (38) and using (27) to get

$$A_k^* = \frac{1}{\omega(1 - \mathrm{e}^{-2\pi \mathrm{i} k\Omega/\omega)}} \oint_{C^*} V_{-k}(\theta')\, \mathrm{e}^{-\mathrm{i}k\Omega\theta'/\omega}\, \mathrm{d}\theta'.$$

On noting that the conjugate contour C^* can be obtained from C by reversing it and translating downwards by $\mathrm{i}\Theta$, and then using the translation symmetry expressed in (26), the result follows. A similar proof is obtained in the case $k = 0$ on conjugating the integral in (39)—note in particular that A_0 is always imaginary (see also (40)).

We are free to choose the integration contour in (15) so that it corresponds to fixing $\theta = \mathrm{i}\Theta/2$ and letting ϕ vary from 0 to 2π (see (16)). Although other choices are possible, this one makes the symmetries of the resulting integral more obvious. Then it is not hard to see as a result of (41) that conjugating the action difference in (24) gives

$$[\Delta G_1(\mathrm{i}\Theta/2, \phi)]^* = \sum_{k=-\infty}^{\infty} -(-1)^{\sigma k} A_k\, \mathrm{e}^{\mathrm{i}k\alpha} = -\Delta G_1(\mathrm{i}\Theta/2, \phi + \sigma\pi).$$

We immediately deduce the following.

(i) If the underlying symmetry is $\mathcal{R}_x$ (so that $\sigma = 0$) then

$$[\Delta G_1(\mathrm{i}\Theta/2, \phi)]^* = -\Delta G_1(\mathrm{i}\Theta/2, \phi)$$

is pure imaginary and the splitting grows or decays exponentially as a function of ε.

(ii) If the underlying symmetry is $\mathcal{R}_{xy}$, then the action difference may have real and imaginary parts that are both nonzero. However, in view of the identity

$$[\Delta G_1(\mathrm{i}\Theta/2, \phi)]^* = -\Delta G_1(\mathrm{i}\Theta/2, \phi + \pi)$$

that holds in that case, the modulation integral in (4) is nevertheless real. The splitting is then an oscillatory function of ε.

(iii) If the perturbation is in addition odd with respect to reflection in y, then the Fourier series has terms with odd k only and $\Delta G_1(\mathrm{i}\Theta/2, \phi)$ is real.

(iv) If the symmetry is $\mathcal{R}_{xy}$ and the perturbation is even with respect to reflection in y, then the Fourier series has terms with even k only and $\Delta G_1(\mathrm{i}\Theta/2, \phi)$ is imaginary. In this case, however, we can alternatively take the underlying symmetry to be $\mathcal{R}_x$ and the physics of the problem is no different from case (i). All that changes is the convention for declaring which states are even or odd.

We summarize the situation by writing the modulation integral in (4) in the form

$$\mathcal{M}(x) = \mathrm{e}^{xf_0}\langle \mathrm{e}^{x(f_1(\phi)+\mathrm{i}f_2(\phi))}\rangle_{\phi\in C_1}, \tag{42}$$

where f_0, $f_1(\phi)$ and $f_2(\phi)$ are all real and

$$f_0 = \mathrm{i}A_0 = \left(\langle H_1\rangle_{(\theta,\phi)\in C_L\times C_1} - \langle H_1\rangle_{(\theta,\phi)\in C_0\times C_1}\right)\tau$$

and

$$\begin{aligned} f_1(\phi) + \mathrm{i}f_2(\phi) &= \sum_{k\neq 0} \mathrm{i}A_k\, \mathrm{e}^{\mathrm{i}k\alpha} \\ &= \sum_{k\neq 0} \frac{i}{\omega(1-\mathrm{e}^{2\pi \mathrm{i}k\Omega/\omega})} \oint_C V_k(\theta')\, \mathrm{e}^{\mathrm{i}k\Omega\theta/\omega}\, \mathrm{d}\theta\, \mathrm{e}^{\mathrm{i}k(\phi-\mathrm{i}\Omega\Theta/(2\omega))} \\ &= -\sum_{k\neq 0} \frac{\mathrm{e}^{\mathrm{i}k\phi}}{2\omega \sin \pi k\Omega/\omega} \oint_C V_k(\theta')\, \mathrm{e}^{\mathrm{i}k\Omega(\theta-\theta_c)/\omega}\, \mathrm{d}\theta, \end{aligned} \tag{43}$$

where $\theta_c = \pi + \mathrm{i}\Theta/2$ is the centre of the unit cell containing the contour C.

When the underlying symmetry is $\mathcal{R}_x$, then $f_2(\phi) = 0$ and the modulation function simplifies to

$$\mathcal{M}(x) = \mathrm{e}^{xf_0}\langle \mathrm{e}^{xf_1(\phi)}\rangle_{\phi\in C_1}.$$

When the underlying symmetry is $\mathcal{R}_{xy}$, then $f_1(\phi)$ and $f_2(\phi)$ are respectively given by the terms with even and odd k in the sum above. Furthermore, if H_1 is an odd function of y, then $f_0 = f_1(\phi) = 0$ and

$$\mathcal{M}(x) = \langle \mathrm{e}^{\mathrm{i}xf_2(\phi)}\rangle_{\phi\in C_1}.$$

4. Some examples

We now apply the calculation of the previous section explicitly to model Hamiltonians, each of them illustrating one of the standard spatial symmetries in two-dimensional problems.

4.1. The quartic double well perturbed by $H_1 = x^2y^2$

We first consider the unperturbed Hamiltonian given in (9). Since the potential in x is a simple quartic and the solution expressible in terms of Jacobi elliptic functions, we can exploit the fact that the only singularities of $x(\theta)$ are simple poles at the centres $\theta_{lm} = (2l+1)\pi + \mathrm{i}(m+1/2)\Theta$ of the unit cells in the complex θ-plane. Around each such pole the Laurent series for $x(\theta)$ begins

$$x(\theta) = (-1)^m\sqrt{2}\mathrm{i}\left(\frac{\omega}{2(\theta-\theta_{lm})} - \frac{\theta-\theta_{lm}}{3\omega} + \cdots\right). \tag{44}$$

In particular, an evaluation of (38) is obtained using the residue calculus centred on $\theta_c = \theta_{11} = \pi + \mathrm{i}\Theta/2$. Here we add the perturbation $H_1 = x^2y^2$ and recall that the underlying symmetry in this case is $\mathcal{R}_x$ and that for this symmetry we have predicted positive splittings with an exponential dependence on the perturbation parameter.

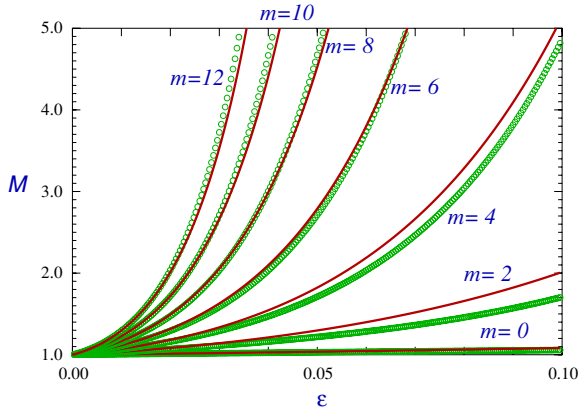

Figure 4. Quantum and semiclassical results for the ratio $\mathcal{M} = \Delta E(\varepsilon)/\Delta E(0)$ are shown for the perturbation $H_1 = x^2y^2$. The continuous curves are the modulation function in (45) and the circles represent quantum data obtained from a numerical diagonalization of the Hamiltonian. These illustrate splittings corresponding to $\Omega = 1, \hbar = 0.05$ and a quantum number for the x degree of freedom of $n = 3$, for which the corresponding one-dimensional mean energy level $E_n = 0.469\ldots$ and the unperturbed splitting is $\Delta E(0) = 8.083\ldots \times 10^{-8}$.

Using the standard expression $y = \sqrt{2J/\Omega}\sin\phi$ relating the action-angle variables of a harmonic oscillator to the position coordinate, we can write $y^2(\phi) = J(1 - \cos 2\phi)/\Omega$, and the oscillating part of the perturbation can be written in the form (19) with

$$V_0(\theta) = \frac{J}{\Omega}\{x^2(\theta)\}$$

and

$$V_{\pm 2}(\theta) = -\frac{Jx^2(\theta)}{2\Omega}$$

and $V_k(\theta) = 0$ for all other k. The terms in the modulation integral (42) can therefore be written more explicitly as

$$f_0 = \mathrm{i}A_0 = \frac{\Theta J}{\Omega\omega}\left[\frac{1}{2\pi}\int_0^{2\pi} x^2(\theta)\,\mathrm{d}\theta - \frac{1}{\mathrm{i}\Theta}\int_0^{\mathrm{i}\Theta} x^2(\theta)\,\mathrm{d}\theta\right]$$

and

$$f_1(\phi) = \sum_{k\neq 0} \mathrm{i}A_k\,\mathrm{e}^{\mathrm{i}k\alpha} = -\frac{\pi J}{\sin 2\pi\Omega/\omega}\cos 2\phi$$

(note that $f_2(\phi) = 0$), where the latter has been evaluated by performing the integral in (43) using the residue calculus. The modulation factor for this perturbation can therefore be written as

$$\mathcal{M}_{x^2y^2}\left(\frac{\varepsilon}{\hbar}\right) = \mathrm{e}^{\varepsilon f_0/\hbar}\frac{1}{2\pi}\int_0^{2\pi} \mathrm{e}^{-z\cos 2\phi}\,\mathrm{d}\phi = \mathrm{e}^{\varepsilon f_0/\hbar} I_0(z), \tag{45}$$

where

$$z = \frac{\pi\varepsilon J}{\hbar\sin 2\pi\Omega/\omega}$$

and $I_0(z)$ is a modified Bessel function.

A comparison between this result and a completely quantum-mechanical numerical calculation is shown in figure 4. To interpret this figure, let n and m respectively be quantum

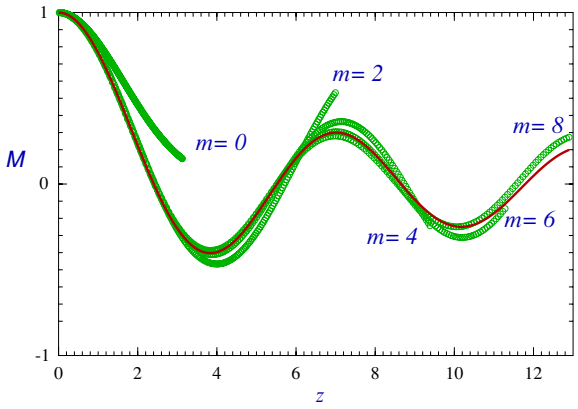

Figure 5. Quantum and semiclassical results for the ratio $\mathcal{M} = \Delta E(\varepsilon)/\Delta E(0)$ are shown for the perturbation $H_1 = xy$, with parameters for the unperturbed problem the same as for the illustration in figure 4. The curve is the modulation function in (45) and the circles represent quantum data. For each value of m we let the value of ε range from 0 to 0.3.

numbers for the x and y degrees of freedom and recall that in the unperturbed problem the splittings are independent of m. The data shown in figure 4 pertain to a set of doublets with a common value $n = 3$ (where $n = 0$ defines the ground state) so that when $\varepsilon = 0$ the splittings for all of these doublets have the same value. As ε increases from 0 these splittings fan out and change differentially with m. The continuous curves in figure 4 represent the uniform semiclassical prediction in (45), in which we set $J = (m + 1/2)\hbar$ and the open circles are exact quantum data. It is evident that the theory developed here provides a good description of the quantum data, even though the quantum numbers involved are not very large.

4.2. The quartic double well perturbed by $H_1 = xy$

We now consider the perturbation $H_1 = xy$, for which the underlying symmetry is $\mathcal{R}_{xy}$. In this case the oscillating part $V(\theta, \phi)$ is simply $H_1(\theta, \phi)$ itself and we have

$$V_{\pm 1}(\theta) = \mp \mathrm{i}\sqrt{\frac{J}{2\Omega}}x(\theta), \tag{46}$$

and $V_k(\theta) = 0$ for $k \neq \pm 1$. Evaluation of (43) by the calculus of residues can once again be achieved on substitution of (44) and this leads to

$$f_2(\phi) = \sum_{k\neq 0} A_k \, \mathrm{e}^{\mathrm{i}k\alpha} = \frac{\pi}{\sin \pi\Omega/\omega}\sqrt{\frac{J}{\Omega}}\cos\phi.$$

The modulation factor is therefore

$$\mathcal{M}_{xy}\left(\frac{\varepsilon}{\hbar}\right) = \frac{1}{2\pi}\int_0^{2\pi} \mathrm{e}^{\mathrm{i}z\cos\phi}\,\mathrm{d}\phi = J_0(z),$$

where

$$z = \frac{\pi\varepsilon}{\hbar \sin \pi\Omega/\omega}\sqrt{\frac{J}{\Omega}}$$

and $J_0(z)$ is a Bessel function (recall that $f_0 = f_1(\phi) = 0$ in this case).

A numerical illustration is shown in figure 5, with parameters in the unperturbed problem the same as used for figure 4. However, we plot the splittings scaled by their unperturbed

value as a function of the parameter z (with the substitution $J = (m + 1/2)\hbar$) rather than of the raw perturbation parameter ε. As predicted by the perturbation calculation, we find that the splittings do indeed oscillate as a function of the perturbation parameter and the splittings that fan out from a given unperturbed splitting depend on $m, \hbar$ and ε largely through the single variable z. In general it is found that the range of perturbation strengths for which the current uniform approximation provides a good description of tunnelling depends on the energy in the x degree of freedom, with the range decreasing as this energy approaches the barrier top [29]. Analytic continuation of the first order perturbative approximation into the complex angle plane evidently fails sooner as the real tori approach the limiting separatrix case and become pinched at the barrier energy. The numerical examples shown here are typical of energies midway between the bottom and barrier of the double well. Closer to the barrier top and for similar values of $\hbar$, the quantum data may part from the modulation integral before a complete oscillation has taken place, although as $\hbar$ decreases multiple oscillations are again revealed (for comparable torus actions). The range of z over which the modulation integral provides a correct description of the splitting increases as $\hbar$ decreases [29], although this may at the same time correspond to a decreasing range in the raw perturbation parameter ε. The range also depends of course on other parameters such as Ω (which controls proximity to resonance). A calculation to higher order in perturbation theory, which has not been performed, would be useful for better understanding the limitations in the applicability of the current approximation.

4.3. Pendulum Hamiltonians

Although the derivation of the splitting was presented for the special case of tori separated by a potential barrier in configuration space, the results are canonically invariant and should apply more generally. We illustrate this here by considering a pendulum Hamiltonian in one degree of freedom coupled to a harmonic oscillator in another. The unperturbed Hamiltonian is

$$H_0 = \tfrac{1}{2}p_x^2 + \tfrac{1}{2}p_y^2 + \cos x + \tfrac{1}{2}\Omega^2 y^2$$

and we consider perturbation by

$$H_1 = \varepsilon p_x p_y,$$

for which the underlying symmetry is of type $\mathcal{R}_{xy}$. This particular perturbation is chosen for the convenience of numerical quantum calculations rather than for any special features of the semiclassical calculation. We note that pendulum Hamiltonians are useful models of resonances in generic near-integrable problems and the sort of application illustrated here may be important for quantitative treatments of resonance-assisted tunnelling [12].

We consider energies greater than the separatrix energy $E = 1$ of the pendulum. In this case tunnelling is between tori for which momentum p_x rather than position x has different sign. If we zero the x-angle θ of the unperturbed problem at the point $x = 0$ and $p_x = -\sqrt{2(E-1)} < 0$, then the discussion of section 2.1 carries over essentially unaltered except for the fact that the real tori λ_L and λ_R are characterized by different signs of p_x rather than of x. Starting from $\theta = 0$, integration in imaginary θ defines a periodic orbit whose period in θ we denote by $2\mathrm{i}\Theta$. It cycles between λ_L and λ_R and is such that $x(\theta + \mathrm{i}\Theta) = -x(\theta)$ and $x(\theta)$ is once again a biperiodic function of the type illustrated at the left of figure 1. The symmetries $\mathcal{R}_x$ and $\mathcal{R}_{xy}$ act on angle variables according to the form given in (12). The pendulum analogue of the right half of figure 1 is given in figure 6.

The one-dimensional solutions for $(x(\theta), p_x(\theta))$ can once again be written in terms of Jacobi elliptic functions (see [31] for example) and one can show in particular that the

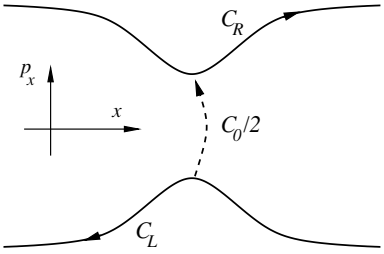

Figure 6. The boundaries if the unit cell in the complex angle plane also map to real and complex orbits, as shown schematically here in a phase plane, in the case of a pendulum Hamiltonian.

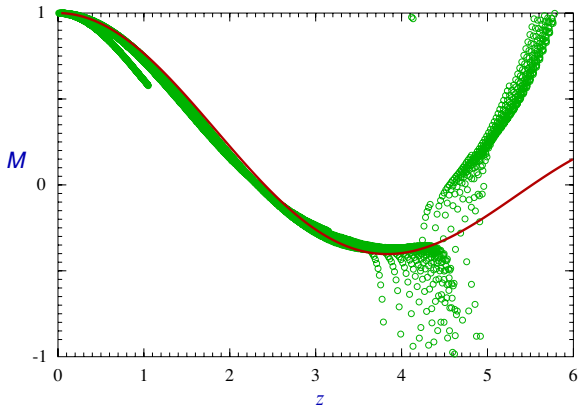

Figure 7. Quantum and semiclassical results for the ratio $\mathcal{M} = \Delta E(\varepsilon)/\Delta E(0)$ are shown for the perturbation $H_1 = p_x p_y$ of the pendulum Hamiltonian with $\Omega = 1$ and $\hbar = 0.04$. The data correspond to states whose energy in the x degree of freedom is $E_n = 1.2711\ldots$, the sixth level above the separatrix energy, and whose splittings have the common value $\Delta E(0) = 1.356\ldots \times 10^{-9}$ in the unperturbed limit. Except for the case $m = 0$, which falls visibly below the theoretical prediction for $z < 1$, it is not possible to distinguish data for different values of m in this case and we have not labelled them here.

singularities of $p_x(\theta)$ are simple poles at the centres of the unit cells, around each of which we have the Laurent series

$$p_x(\theta) = (-1)^m i \left(\frac{2\omega}{\theta - \theta_{lm}} + \frac{\theta - \theta_{lm}}{3\omega} + \cdots \right).$$

Inserting

$$V_{\pm 1}(\theta) = \sqrt{\frac{\Omega J}{2}}\, p_x(\theta)$$

in (43) and evaluating the contour integral using the calculus of residues gives

$$f_2(\phi) = \frac{2\pi\sqrt{2\Omega J}}{\sin \pi\Omega/\omega} \sin\phi$$

(and $f_0 = f_1(\phi) = 0$). The modulation factor

$$\mathcal{M}_{p_x p_y}\left(\frac{\varepsilon}{\hbar}\right) = J_0(z)$$

in this case is therefore the same as that found in the xy perturbation of the quartic oscillator, up to a numerical factor in the argument

$$z = \frac{2\pi\sqrt{2\Omega J}\varepsilon}{\hbar \sin \pi\Omega/\omega}$$

of the Bessel function.

A numerical illustration of this result, analogous to figure 5, is shown in figure 7. Here we have once again plotted the ratio $\mathcal{M} = \Delta E(\varepsilon)/\Delta E(0)$ as a function of the parameter z for a collection of states with a common quantum number in the x degree of freedom. In this illustration we see that the semiclassical approximation describes the computed splittings over the first sign change but not for several oscillations as we had in the illustration used for the case of the quartic oscillator. As in previous cases, the range of z over which the perturbative approximation gives a good description of the data is found to depend on parameters such as Ω proximity to the separatrix energy in the x degree of freedom, and, of course, $\hbar$.

5. Conclusion

We have shown that the essential qualitative behaviour of tunnel splittings in near-integrable systems can be captured by a semiclassical approximation which incorporates perturbative approximation of the complexified invariant tori. In two-dimensional potentials, regimes corresponding to two distinct symmetry types have been illustrated. In the case where the symmetry is of reflection in one coordinate we find that splittings remain positive and vary exponentially with parameters. When the underlying symmetry is inversion through a point, however, splittings oscillate as a function of parameters and can change sign and even vanish at certain parameter values.

The essential mechanism underlying the change from integrable to near-integrable behaviour is a breaking of global symmetry in the complexified torus. While analytic continuation of two congruent tori leads to identical complex manifolds in the integrable case, in near-integrable problems the corresponding analytic continuations are distinct. We remark that an analogous symmetry breaking occurs in the toral structure underlying resonant states in metastable wells. In that case, however, breaking integrability introduces a distinction between a continued torus and its complex conjugate rather than between 'left' and 'right' tori as in splitting calculations. A real torus corresponding to bound motion in an exactly integrable metastable well will, when continued across a barrier, define a real manifold of orbits escaping to infinity. A perturbative calculation such as used here indicates that a small perturbation turns that real manifold slightly complex on the unbound side of the barrier. The corresponding wavefunction would therefore exhibit a strong directionality due to the fact that the resulting action variations have a nonzero imaginary part, which is a feature not seen in exactly integrable systems. This mechanism could well lead to strong directionality in the emission patterns of slightly nonspherical optical resonators similar to that recently reported in [32–34].

Finally, we emphasize that the ability of the perturbation calculation here to describe splittings arises despite the fact that the exact classical data underlying (2) are not strictly defined due to the intervention of natural boundaries. An important question which this work has not addressed is at what point, as $\hbar$ decreases for fixed ε or as ε increases for fixed $\hbar$ for example, (2) fails entirely to give a description of tunnelling because the underlying classical geometry cannot be described exactly. A better understanding of this issue should come from working to higher order in perturbation theory although the ensuing calculation would be more cumbersome to implement than the one we have done.

Acknowledgments

GS was supported by an EPSRC studentship.

Appendix. Derivation of the splitting formula

In this appendix we provide some additional detail regarding the derivation of the splitting formula (15) from Herring's integral. We insert the WKB approximations for the quasimodes ψ_L and ψ_R in the integral and retain only the diagonal terms in the resulting sum over branches since the off-diagonal terms have rapidly varying phase and contribute negligibly to the integral. The density functions in the amplitudes of ψ_L and ψ_R have the form

$$\rho_{L,R} = \frac{1}{2\pi} \left. \frac{\partial(\theta, \phi)}{\partial(n, s)} \right|_{\lambda_{L,R}}$$

and we approximate these by their unperturbed values. Taking advantage of the fact that λ_L^* and λ_R are actually the same manifold in the unperturbed problem, the Herring integral can therefore be written approximately in the form

$$\Delta E \approx \sum_{\text{branches}} \frac{\hbar}{2\pi^2} \int_\Gamma \mathcal{A}\, \mathrm{e}^{\mathrm{i}(S_L - S_R^*)/\hbar}\, \mathrm{d}s, \tag{A.1}$$

where the amplitude can be written as

$$\mathcal{A} = \dot{n} \frac{\partial(\theta, \phi)}{\partial(n, s)}$$

and where $\dot{n}$ is the rate of change of n along an orbit on the complex torus with position (n, s) (and arises from the normal derivative of the phase functions on λ_L^* and λ_R). We simplify this amplitude term further by rewriting it using the new angle-like variables (α, t) defined in (14). We note that $\dot{t} = 1$ and that α is constant on each individual orbit. We can therefore write

$$\dot{n} = \left(\frac{\partial n}{\partial t} \right)_\alpha = \frac{\partial(n, \alpha)}{\partial(t, \alpha)},$$

where the subscript α indicates that the variable is held fixed in the partial derivative. Repeated use of the chain rule then allows one to simplify the amplitude $\mathcal{A}$ as follows:

$$\mathcal{A} = \frac{\partial(\theta, \phi)}{\partial(t, \alpha)} \frac{\partial(n, \alpha)}{\partial(n, s)} = \omega \left(\frac{\partial \alpha}{\partial s} \right)_n = \omega \left(\frac{\partial \alpha}{\partial s} \right)_\Gamma.$$

This enables us to convert the sum over branches and integral with respect to s into a simple integral with respect to α according to

$$\sum_{\text{branches}} \int_\Gamma \mathcal{A}\, \mathrm{d}s \to \omega \int_0^{2\pi} \mathrm{d}\alpha$$

and the Herring integral then reduces to (15), as required.

References

[1] Berry M V and Mount K E 1972 *Rep. Prog. Phys.* **35** 315
[2] Wilkinson M 1986 *Physica* D **21** 341
[3] Takada S, Walker P N and Wilkinson M 1995 *Phys. Rev.* A **52** 3546
[4] Takada S 1996 *J. Chem. Phys.* **104** 3742
[5] Creagh S C 1998 *Tunneling in Complex Systems* ed S Tomsovic (Singapore: World Scientific)
[6] Creagh S C and Finn M D 2001 *J. Phys. A: Math. Gen.* **34** 3791

[7] Percival I C and Greene J M 1981 *Physica* D **3** 530
[8] Percival I C 1982 *Physica* D **6** 67
[9] Billi L, Turchetti G and Xie R 1993 *Phys. Rev. Lett.* **71** 2513
[10] Bohigas O, Tomsovic S and Ullmo D 1993 *Phys. Rep.* **223** 45
[11] Tomsovic S and Ullmo D 1994 *Phys. Rev.* E **50** 145
[12] Brodier O, Schlagheck P and Ullmo D 2001 *Phys. Rev. Lett.* **87** 064101
[13] Brodier O, Schlagheck P and Ullmo D 2002 *Ann. Phys.* **300** 88
[14] Eltschka C and Schlagheck P 2005 *Phys. Rev. Lett.* **94** 014101
[15] Keshavamurthy S 2005 *Phys. Rev.* E **72** 045203
[16] Heisinger W K *et al* 2001 *Nature* **412** 52
[17] Steck D A, Oskay W H and Raizen M G 2001 *Science* **293** 274
[18] Ozorio de Almeida A M 1984 *J. Chem. Phys.* **88** 6139
[19] Tomsovic S, Grinberg M and Ullmo D 1995 *Phys. Rev. Lett.* **75** 4546
[20] Sieber M 1996 *J. Phys. A: Math. Gen.* **29** 4715
[21] Schomerus H and Sieber M 1997 *J. Phys. A: Math. Gen.* **30** 4537
[22] Sieber M and Schomerus H 1998 *J. Phys. A: Math. Gen.* **31** 165
[23] Kaidel J and Brack M 2004 *Phys. Rev.* E **70** 016206
[24] Grossmann F, Dittrich T, Jung P and Hänggi P 1991 *Phys. Rev. Lett.* **67** 516
[25] Grifoni M and Hänggi P 1998 *Phys. Rep.* **304** 229
[26] Creagh S C 1994 *J. Phys. A: Math. Gen.* **27** 4969
[27] Creagh S C and Whelan N D 1999 *Ann. Phys.* **272** 196
[28] Creagh S C 2005 *Nonlinearity* **18** 2089
[29] Smith G C 2005 *PhD Thesis* University of Nottingham
[30] Lichtenberg A J and Lieberman M A 1992 *Regular and Chaotic Dynamics* (New York: Springer)
[31] Dorignacc J and Flach S 2002 *Phys. Rev.* B **65** 214305
[32] Lacey S *et al* 2003 *Phys. Rev. Lett.* **91** 033902
[33] Schwefel H G L *et al* 2004 *J. Opt. Soc. Am.* B **21** 923
[34] Kim S-K *et al* 2004 *Appl. Phys. Lett.* **84** 863